

Supplementary material

Supplementary methods

BrdU administration

BrdU (Sigma-Aldrich) was dissolved in saline at a concentration of 10 mg/mL and sterile-filtered. Mice received an intraperitoneal injection (50 mg/kg) twice daily (8 hours apart) for 3 consecutive days. Cohorts of animals were perfused at 1 day and 22 days after the last BrdU injection to analyze NPC proliferation and NPC survival, respectively.

Behavioural testing

Mice were handled for 7 days prior to behavioural testing. Prior to treatment allocation, we conducted reference testing in nest building and Y maze to allocate mice to subsequent experimental groups in a balanced manner, based on behavioural performance.

Nest building

Nest building activity in mice is a paradigm for activities of daily living. In their homecage, mice were provided with nesting material in the form of pressed cotton pads (3 g total weight), and nest construction was scored after 1, 3, 6 and 24 hours as previously described.⁷⁰ Nests were scored on a scale of 1-5 and unshredded material was weighed at 24 hours.

Marble burying

The marble burying test was used to evaluate anxiety-like behaviour, such that mice with high anxiety engage in more digging in a novel context, and thus bury more marbles.⁷¹ Briefly, mice were placed in individual cages filled 5 cm deep with corn cob bedding, and 20 glass marbles (14 mm diameter) evenly spaced in a 4 × 6 grid arrangement. Mice were left to explore each cage for 30 min, and then the number of marbles submerged (to 2/3 their depth with bedding) or fully buried were counted.

Open field test

Exploratory and locomotor activity was measured in the open field test. Mice were positioned in the center of a white, acrylic plastic, square-shaped arena (45 cm × 45 cm × 45 cm) for 10 min on 3 consecutive days. The arena was illuminated by a bulb placed above the center of the maze (150 lux field center). The field was cleaned with 70% ethanol after each trial. All data was video recorded and analyzed using Ethovision XT (Noldus). Total distance travelled, time spent in different areas of the field (i.e. center vs periphery) and number of rearing events were calculated.

Novel object recognition task

The NOR test was used to study recognition memory. Mice explored two identical objects in the open field arena in a 10 min habituation trial, which was followed by a 10 min retention trial, where one of the familiar objects was replaced by an unfamiliar one. The trials were separated by a 1-hour inter-trial interval, during which mice were placed in their homecage. The objects (i.e. red plastic cup, glass beaker filled with bedding material) differed in size, material, shape, and color. The test arena was cleaned with 70% ethanol after each trial. Data was video recorded and analyzed using Ethovision XT (Noldus). The duration of object exploration (i.e. nose directed toward and within 1cm of the object) was recorded. Sitting on an object was not classified as exploratory behaviour. Memory index was calculated as: (time spent exploring the novel object – time spent exploring the familiar object)/total exploration time.

Y maze

Spatial working memory was evaluated using the Y maze. The apparatus, made of white acrylic plastic, has three identical arms (40 cm × 8 cm × 16 cm) spaced 120° with respect to each other that converge on a central triangular platform. Illumination was maintained at 150 lux at the maze center. Mice were habituated to the apparatus by exploring one of the arms for 5 min. During testing, mice were placed at the end of one of the arms and allowed to explore all 3 arms for 8 min. The maze was cleaned with 70% ethanol between trial. Data was recorded and analyzed with Ethovision XT (Noldus). Percent alternation was calculated as: consecutive entries in all 3 arms/total alternations.

Barnes maze

The Barnes maze task was used to assess spatial learning and memory. A white circular table with the following specifications was used: 105 cm high; 92 cm diameter; 20 identical holes with a diameter of 5 cm equally distributed around the perimeter of the table; one hole (i.e. target hole) connected to an escape box. In a single-trial habituation phase, the animal was placed in a clear cylinder in the maze center for 10 s. The cylinder was then used to guide the mouse until it was located above the target hole. Mice that did not find the target hole within 1 min were gently guided into the escape box. All mice were left in the escape chamber for 1 min before being returned to their homecage. During the acquisition phase, 4 different visual cues were placed on the walls around the Barnes Maze. Mice were trained over 4 days (300 s per trial, 2 daily trials, 40 min inter-trial interval) to find the target hole. Each trial began with the mouse placed in an opaque box positioned in the center of the maze for 10 s. Mice that did not find the target hole were guided to it. All mice were left in the escape box for 1 min. An overhead light (800 lux at the center of the maze) and buzzer was used during each trial to motivate escape in the Barnes maze. After the acquisition phase, mice were tested in a probe trial with closed holes for 300 s. Following the probe test, a reversal learning phase was used to test cognitive flexibility, in which the target hole was repositioned 180° from the original location. Mice were given 4 days (300 s per trial, 2 daily trials, 40 min inter-trial interval) to find the new target hole, followed by another probe test 24 hour later. Between trials, the maze and holes were wiped with 70% ethanol and randomly rotated to dissipate odor cues, and the maze was rotated between trials to eliminate the use of intra-maze cues. Video tracking software (Ethovision XT, Noldus) was used to calculate the latency to reach the target hole, total distance travelled and mean speed. Target hole exploration was evaluated during the probe test as the percentage of time spent in the target zone. Errors were defined as the number of entries in a non-target hole. Search strategies during acquisition, reversal and probe trials were classified as previously described.⁷²

Imaging analysis

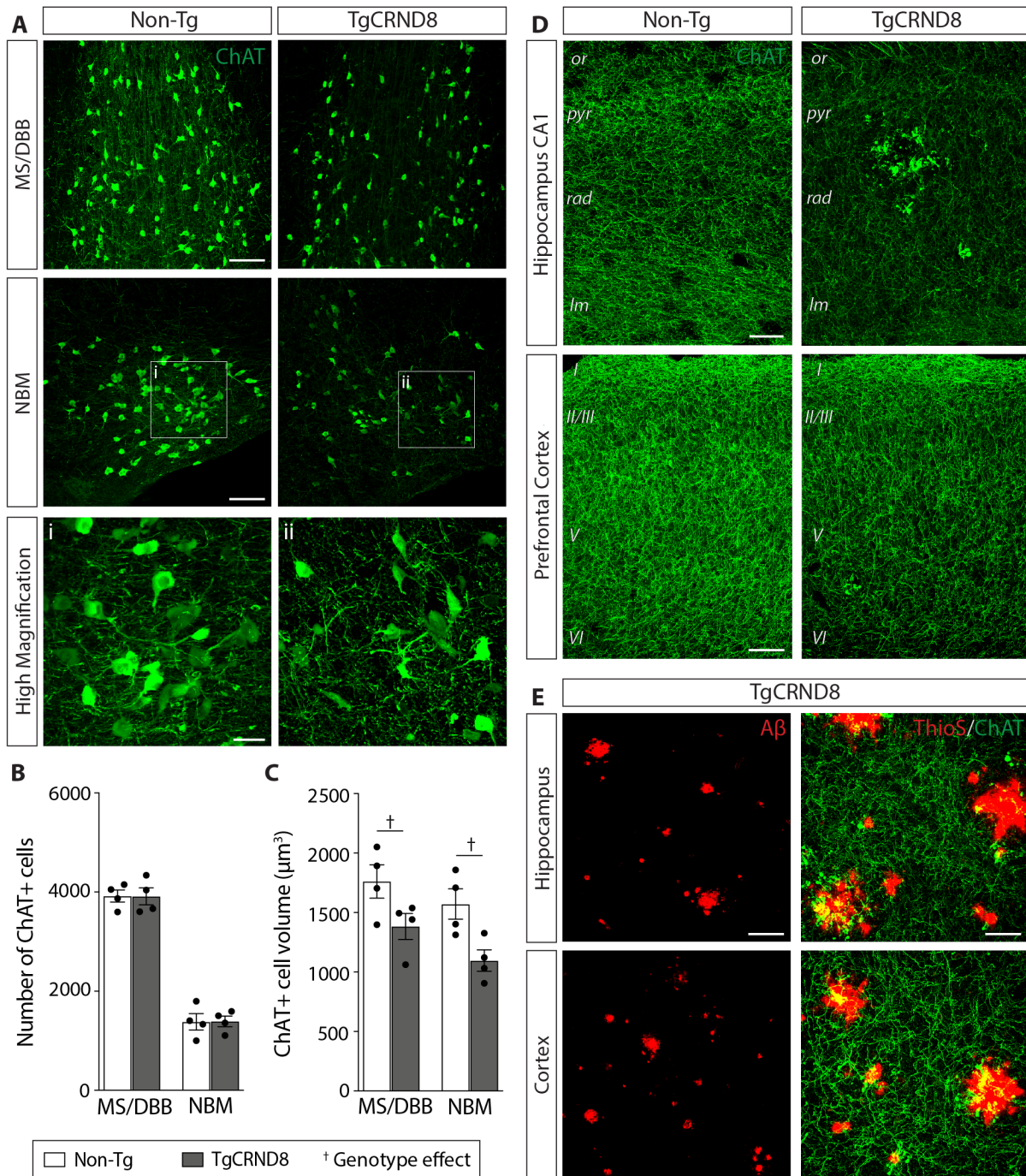
ChAT immunolabeling was imaged with a 20X objective. Every sixth section throughout MS/DBB and NBM subregions of the basal forebrain was immunostained, ChAT+ cells were counted, and the sum of counts multiplied by 6 to obtain an estimate of total numbers per brain region. In every third field, cells were used for neuron reconstruction with Neurolucida software (MBF

Bioscience). Soma volume, neurite length, surface area, and branching order were calculated using NeuroLucida Branched Structure Analysis. ChAT+ fiber density was quantified in 3 sections per animal using Hessian-based filter and line intensity scan analysis as previously described.⁷³

BrdU+, BrdU/NeuN+, BrdU/DCX+ cells in the dentate were imaged using a 20X objective. Sections were systematically sampled 1-in-12 for staining, and cells were counted and multiplied by the series interval to estimate total numbers. For co-labelling analysis, the phenotype of identified BrdU+ were analyzed, and expressed as the proportion of BrdU+ cells co-labelled with DCX or NeuN. DCX+ dendrites oriented vertically in the GCL were traced. A minimum of 36 cells per group from at 6 animals were quantified. NeuroLucida Branched Structure Analysis was used to calculate total dendritic length and apical dendrite length. NeuroLucida Sholl Analysis was used to characterize the dendritic branching pattern (i.e. the number of intersections of dendrites with concentric circles as a function of distance from the soma).

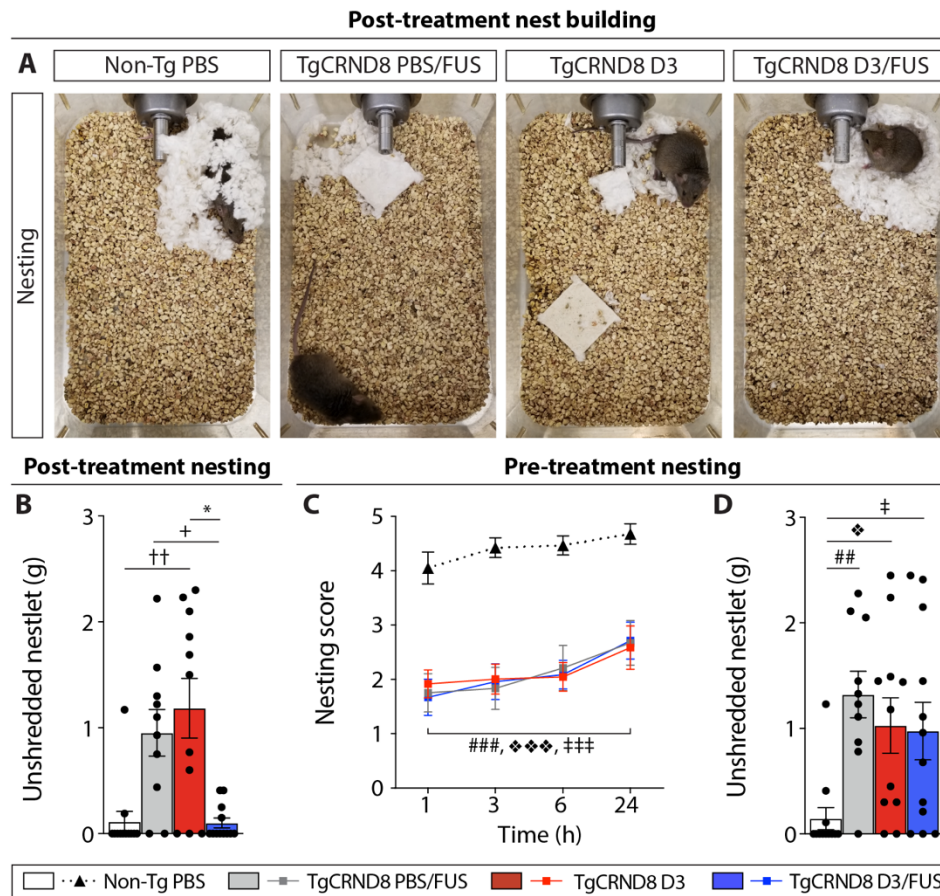
To assess amyloid deposition, a 1-in-12 series of brain sections from each animal was probed with the A β -specific antibody 6F3D and imaged at 10X magnification. ImageJ Particle Analysis was used to calculate plaque number, mean size, and surface area as previously described.²⁶ A set threshold was applied to all images and deposits of at least 25 μm^2 were included for analysis. ChAT and Thioflavin S staining were visualized with a 10X objective. For each brain region, a 1-in-12 series of sections per animal was imaged. Clusters of ChAT-stained dystrophic neurites and Thioflavin S staining were traced in ImageJ via histogram thresholding to compute the immunopositive area.

Supplementary figures



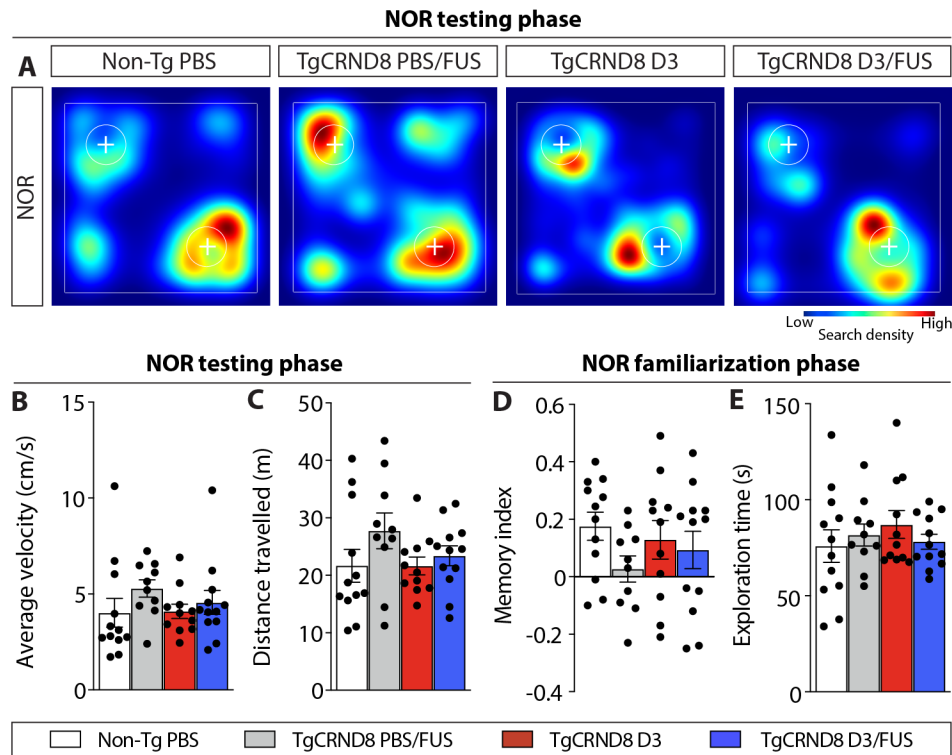
Supplementary Figure 1 Cholinergic deficits and amyloid plaque pathology in 5-month-old TgCRND8 mice. (A) Representative confocal images of ChAT⁺ neurons in the MS/DBB and NBM of non-Tg and TgCRND8 mice. (B) Relative to non-Tg controls, 5-month-old TgCRND8 mice have comparable numbers of ChAT⁺ neurons in the basal forebrain, and (C) decreased

ChAT+ cell volume. **(D)** Qualitative observations revealed reduced cholinergic fibre innervation in the hippocampus and cortex of TgCRND8 mice compared to non-Tg mice. **(E)** Extensive amyloid pathology and ChAT+ dystrophic neurites surrounding the plaque core are present by 5 months of age. Scale bars: (A, D) 100 μm ; (i,ii) 30 μm , (E) left column = 100 μm , right column = 30 μm . Statistics: One-way ANOVA with Holm-Sidak post-hoc test. Significance: † $P < 0.05$; ‡ indicates comparison of TgCRND8 mice with non-Tg mice (genotype effect). Data represent means \pm SEM; $n=4$ per group.



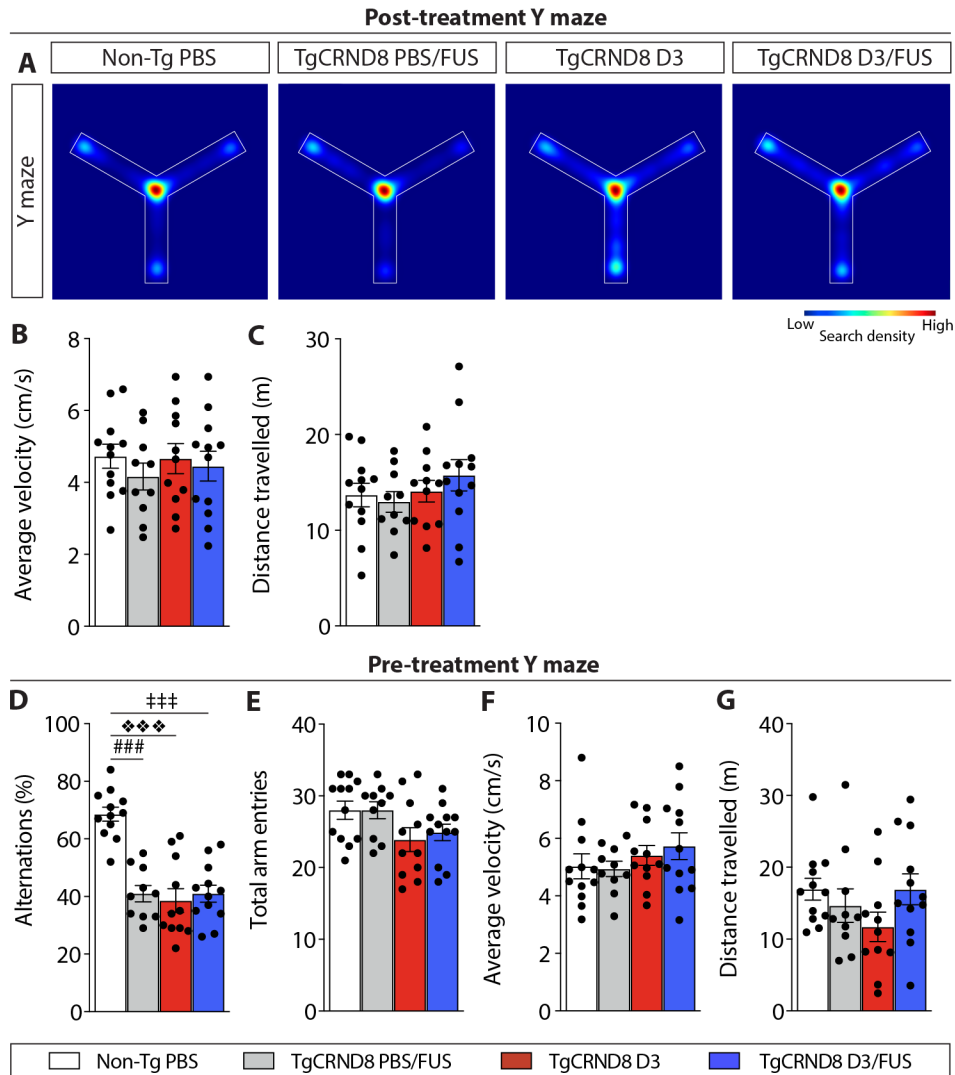
Supplementary Figure 2 MRIgFUS-mediated delivery of D3 rescues nest building behaviour in TgCRND8 mice. **(A)** Representative nest construction after 24 hours in PBS-treated non-Tg mice, PBS/FUS, D3 and D3/FUS-treated TgCRND8 mice. **(B)** D3-treated TgCRND8 mice had significantly more unshredded nest material at the end of the testing period compared to non-Tg mice and D3/FUS-treated TgCRND8 mice. Nest shredding was improved in D3/FUS relative to PBS/FUS-treated TgCRND8 mice. **(C)** Pre-treatment nest construction and **(D)** unshredded nestlet

weight were comparable across TgCRND8 mice allocated to PBS/FUS, D3 and D3/FUS treatment groups. (B, D) Kruskal-Wallis test with Dunn's post hoc test or (C) Repeated measures ANOVA with Holm-Sidak post hoc test. Significance: *,+,‡,❖ $P < 0.05$; ††, ## $P < 0.01$; ###,†††,❖❖❖ $P < 0.001$; for analysis of post-treatment nesting, † indicates comparison of D3-treated TgCRND8 mice with PBS-treated non-Tg mice (genotype effect); + indicates comparison of PBS/FUS-treated with D3/FUS-treated TgCRND8 mice (D3 effect); * indicates comparison of D3-treated with D3/FUS-treated TgCRND8 mice (D3/FUS effect); for analysis of pre-treatment nesting, # indicates comparison of PBS/FUS-allocated TgCRND8 mice with non-Tg mice; ❖ indicates comparison of D3-allocated TgCRND8 mice with non-Tg mice; ‡ indicates comparison of D3/FUS-allocated TgCRND8 mice with non-Tg mice. Data represent means \pm SEM; $n = 10-12$ per group.



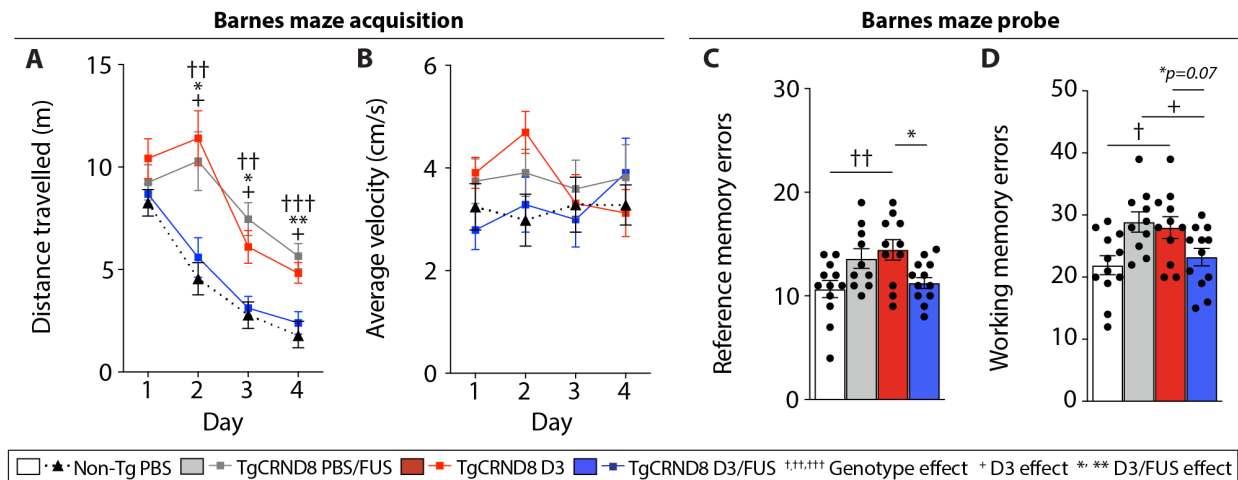
Supplementary Figure 3 MRIgFUS-mediated delivery of D3 promotes recognition memory task performance in TgCRND8 mice. (A) Representative heat maps of search density surrounding the familiar object (top left) and novel object (bottom right) in PBS-treated non-Tg mice, PBS/FUS, D3 and D3/FUS-treated TgCRND8 mice during the NOR test. D3/FUS treated mice displayed a preference for the novel object relative to D3 and PBS/FUS-treated TgCRND8

mice, similar to non-Tg controls. **(B)** During the novel object testing phase, no alterations in motor function were observed as measured by average velocity, and **(C)** total distance travelled. **(D)** In the familiarization session with two identical objects, the memory index, and **(E)** time spent exploring the objects were comparable across treatment groups. Statistics: (B-E) One-way ANOVA with Holm-Sidak post hoc test. Data represent means \pm SEM; n=10-12 per group.

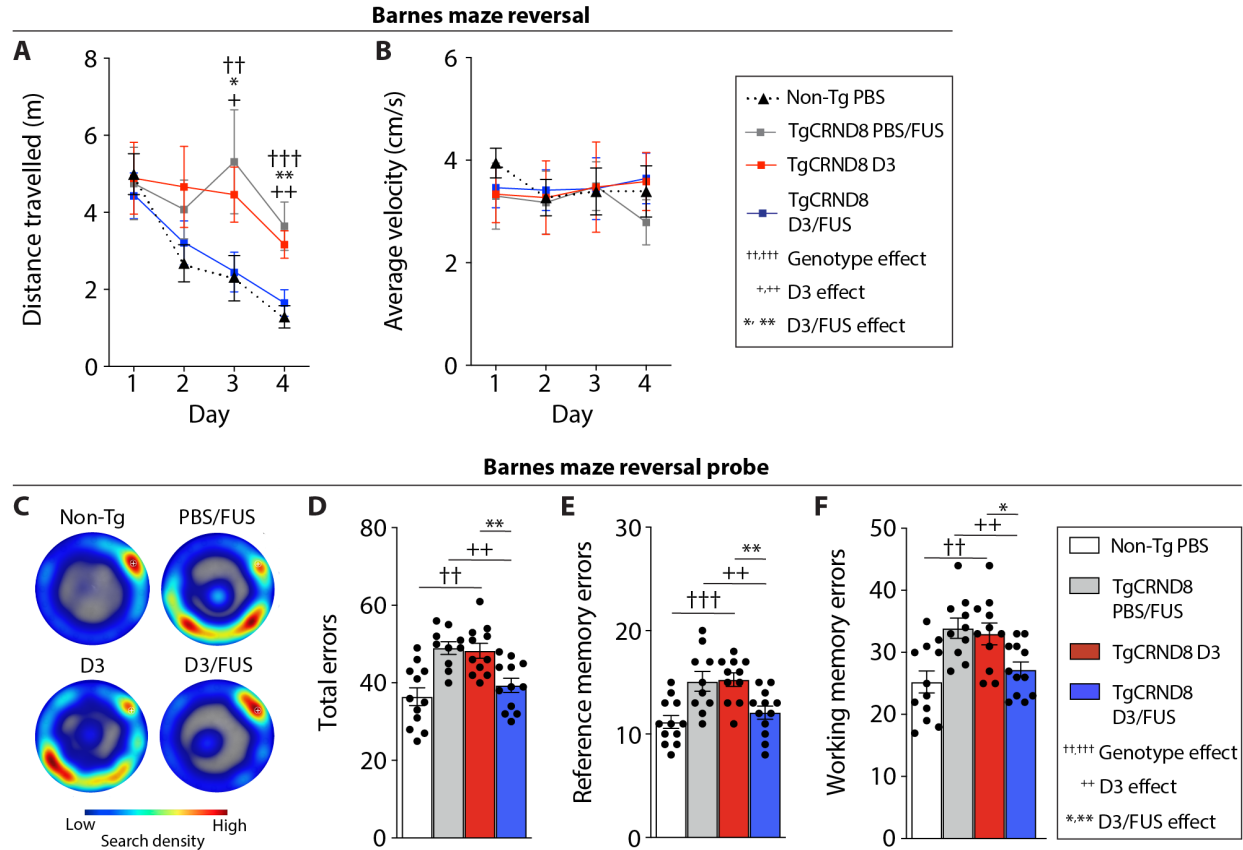


Supplementary Figure 4 Spatial working memory in the Y maze in TgCRND8 mice. **(A)** Representative heat maps of search density in the Y maze in PBS-treated non-Tg mice, PBS/FUS, D3 and D3/FUS-treated TgCRND8 mice revealed comparable exploration time in all three arms during testing. **(B)** Motor function as measured by average velocity and **(C)** distance travelled was comparable across treatment groups during the Y maze task. **(D)** Prior to treatment, TgCRND8

allocated to PBS/FUS, D3 and D3/FUS experimental groups all demonstrated fewer alternations relative to non-Tg mice. **(E)** The total number of arm entries were similar in all treatment conditions. **(F)** At baseline, no change in locomotor behaviour was observed as measured by average velocity, and **(G)** total distance travelled. Statistics: (B-G) One-way ANOVA with Holm-Sidak post hoc test. Significance: ###,###, ❖❖❖ $P < 0.001$; # indicates comparison of PBS/FUS-allocated TgCRND8 mice with non-Tg mice; ❖ indicates comparison of D3-allocated TgCRND8 mice with non-Tg mice; † indicates comparison of D3/FUS-allocated TgCRND8 mice with non-Tg mice. Data represent means \pm SEM; $n=10-12$ per group.

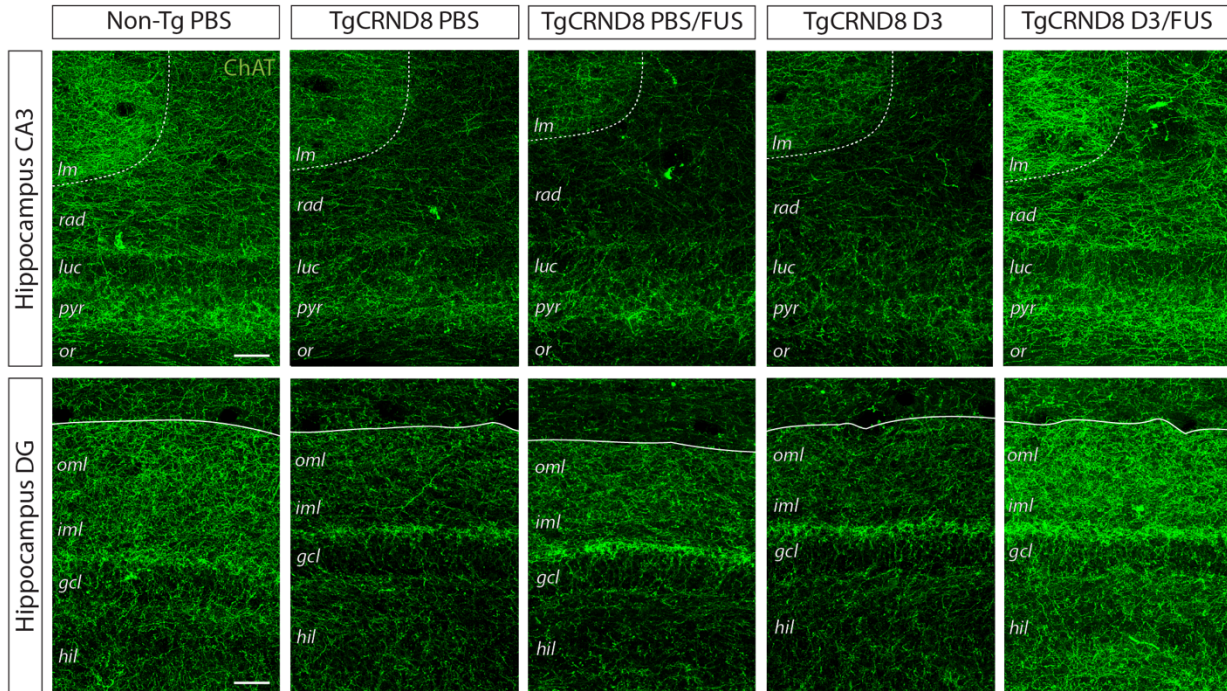


Supplementary Figure 5 MRIgFUS-mediated delivery of D3 in TgCRND8 mice promotes spatial learning and memory performance in the Barnes maze. (A) D3/FUS-treated TgCRND8 mice travelled less to reach their target compared to D3 and PBS/FUS-treated TgCRND8 mice. **(B)** Average velocity was comparable across treatment groups during the acquisition trials. **(C)** In the probe trial, the number of reference memory errors (i.e. first entry into a non-target hole) and **(D)** working memory errors (i.e. additional entries to non-target holes) were decreased in D3/FUS-treated relative to D3-treated TgCRND8 mice. Statistics: (A, B) Repeated measures or (C, D) one-way ANOVA with Holm-Sidak post hoc test. Significance: *,+,† $P < 0.05$; **,†† $P < 0.01$, ††† $P < 0.001$; † indicates comparison of D3-treated TgCRND8 mice with PBS-treated non-Tg mice (genotype effect); + indicates comparison of PBS/FUS-treated with D3/FUS-treated TgCRND8 mice (D3 effect); * indicates comparison of D3-treated with D3/FUS-treated TgCRND8 mice (D3/FUS effect). Data represent means \pm SEM; $n=10-12$ per group.

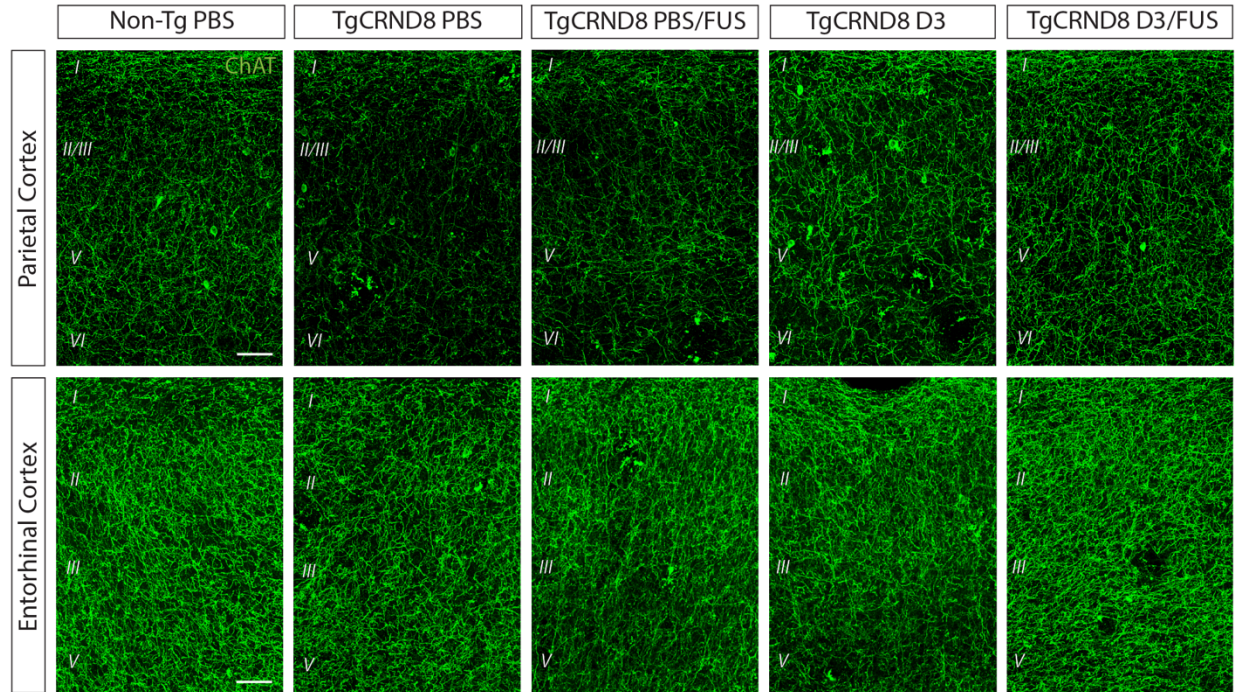


Supplementary Figure 6 MRIGFUS-mediated delivery of D3 in TgCRND8 mice improves cognitive flexibility in the Barnes maze. (A) In the reversal phase of the Barnes maze, D3/FUS-treated mice displayed a faster learning curve compared to D3 and PBS/FUS-treated mice as measured by total distance travelled, comparable to non-Tg controls. (B) Locomotion as measured by average velocity was comparable across treatment groups during the learning trials. (C) Representative heat maps of search density during the reversal probe trial demonstrate that D3-treated and PBS/FUS-treated TgCRND8 mice spent less time near the target hole in the absence of the escape box compared to D3/FUS treated TgCRND8 mice and non-Tg controls. (D) TgCRND8 mice treated with D3/FUS entered fewer non-target holes (errors), (E) reference memory errors (i.e. first entry into a non-target hole) and (F) working memory errors (i.e. additional entries to non-target holes) compared to PBS/FUS and D3-treated TgCRND8 mice, similar to non-Tg levels. Statistics: (A, B) Repeated measures or (D-F) one-way ANOVA with Holm-Sidak post hoc test. Significance: *,+ $P < 0.05$; **,++,††† $P < 0.01$, †††† $P < 0.001$; † indicates comparison of D3-treated TgCRND8 mice with PBS-treated non-Tg mice (genotype effect); +

indicates comparison of PBS/FUS-treated with D3/FUS-treated TgCRND8 mice (D3 effect); * indicates comparison of D3-treated with D3/FUS-treated TgCRND8 mice (D3/FUS effect). Data represent means \pm SEM; n=10-12 per group.



Supplementary Figure 7 Hippocampal cholinergic fiber innervation in TgCRND8 mice following D3/FUS treatment. Representative confocal images of ChAT-stained (green) hippocampi showing cholinergic fiber density in PBS-treated non-Tg mice, PBS, PBS/FUS, D3 and D3/FUS-treated TgCRND8 mice. Qualitative observations in PBS-treated TgCRND8 mice indicate reduced cholinergic innervation in the CA3 and DG subfields of the hippocampus relative to age-matched non-Tg mice. The density of ChAT+ fibers in the presence of D3/FUS in TgCRND8 mice appeared similar to non-Tg mice, and of greater abundance compared to PBS, PBS/FUS and D3 TgCRND8 controls. Scale bar: 50 μ m. or: stratum oriens; pyr: stratum pyrimidale; luc: stratum lucidum; rad: stratum radiatum; lm: stratum lacunosum moleculare; oml: outer molecular layer; iml: inner molecular layer; gcl: granule cell layer; hil: hilus.



Supplementary Figure 8 Cholinergic fiber innervation in the parietal cortex and entorhinal cortex of TgCRND8 mice following D3/FUS treatment. Representative confocal images of ChAT-stained (green) cortical regions showing cholinergic fiber density in PBS-treated non-Tg mice, PBS, PBS/FUS, D3 and D3/FUS-treated TgCRND8 mice. Cholinergic innervation in the parietal cortex and entorhinal cortex of TgCRND8 PBS mice appeared reduced relative to age-matched non-Tg PBS mice. In contrast, such differences were not evident in TgCRND8 D3/FUS mice. Scale bar: 50 μ m.